

# PhiReX: a programmable and red light-regulated protein expression switch for yeast

Lena Hochrein<sup>1</sup>, Fabian Machens<sup>1</sup>, Katrin Messerschmidt<sup>1</sup> and Bernd Mueller-Roeber<sup>2,3,\*</sup>

<sup>1</sup>University of Potsdam, Cell2Fab Research Unit, Karl-Liebknecht-Str. 24–25, 14476 Potsdam, Germany, <sup>2</sup>University of Potsdam, Department of Molecular Biology, Karl-Liebknecht-Str. 24–25, 14476 Potsdam, Germany and <sup>3</sup>Max Planck Institute of Molecular Plant Physiology, Am Mühlenberg 1, 14476 Potsdam, Germany

Received April 20, 2017; Revised July 03, 2017; Editorial Decision July 04, 2017; Accepted July 05, 2017

## ABSTRACT

**Highly regulated induction systems enabling dose-dependent and reversible fine-tuning of protein expression output are beneficial for engineering complex biosynthetic pathways. To address this, we developed PhiReX, a novel red/far-red light-regulated protein expression system for use in *Saccharomyces cerevisiae*. PhiReX is based on the combination of a customizable synTALE DNA-binding domain, the VP64 activation domain and the light-sensitive dimerization of the photoreceptor PhyB and its interacting partner PIF3 from *Arabidopsis thaliana*. Robust gene expression and high protein levels are achieved by combining genome integrated red light-sensing components with an episomal high-copy reporter construct. The gene of interest as well as the synTALE DNA-binding domain can be easily exchanged, allowing the flexible regulation of any desired gene by targeting endogenous or heterologous promoter regions. To allow low-cost induction of gene expression for industrial fermentation processes, we engineered yeast to endogenously produce the chromophore required for the effective dimerization of PhyB and PIF3. Time course experiments demonstrate high-level induction over a period of at least 48 h.**

## INTRODUCTION

In recent years, *Saccharomyces cerevisiae* has proven to be a valuable host for diverse synthetic biology applications. Examples range from the production of medically relevant substances like taxadiene (1), artemisinic acid (2) or opioids (3) to compounds of technical importance, e.g. biofuels (4–6). Efficient protein production often requires robust molecular tools for the transcriptional regulation of both, heterologous and endogenous genes.

Chemically inducible promoters, available in a large number in yeast (7–12), do not satisfy the high demands of synthetic biology: reversible or dose-dependent induction is in most cases not easily accomplished and certain chemicals are expensive or show toxic effects in higher concentrations. To overcome these drawbacks, different light-responsive expression systems have been implemented in *S. cerevisiae*, mostly based on plant-derived optical dimerizers, which allow joining a DNA-binding domain (DBD) and a transcriptional activation domain (AD) upon light application (13–16). However, none of the previously reported light-inducible expression systems for yeast allows programmable targeting of DNA-binding sites (DBS), which is a requirement for the orthogonal regulation and the specific control of endogenous genes. Chemically inducible synthetic transcription factors (synTFs) with customizable DBDs based on zinc finger proteins (ZFPs), transcription activator like effectors (TALEs) or CRISPR/Cas9 have previously been reported in yeast (17–19).

To fill this gap, we developed PhiReX (Programmable, highly inducible Red light eXpression system). The system is based on the photoreceptor PhyB and its interacting partner, the helix-loop-helix protein PIF3 from *Arabidopsis thaliana* (13). The photoreceptor binds to a chromophore, which triggers a photon-dependent switch between two conformations: the red light ( $\lambda = 660$  nm) absorbing Pr form and the far-red light ( $\lambda = 730$  nm) absorbing Pfr form. The active PhyB Pfr dimerizes specifically with PIF3 (20). This interaction can be used to design light-sensitive synTFs whereby the programmable DBD of a synthetic TALE (synTALE) is fused to PhyB, and an AD is fused to PIF3. TALEs are natural type III effector proteins secreted by *Xanthomonas sp.* and contain a region consisting of highly conserved tandem repeat modules, each usually 34 amino acids (aa) long (21). Positions 12 and 13 of each repeat module, the so-called repeat variable di-residues (RVDs), are hypervariable. Recent studies showed a strong correlation between unique RVDs and the corresponding nucleotide in the targeted DBS. This results in a simple code that allows predicting the DNA-target site for any given combination of RVDs (22,23). Consequently, it is possible to design

\*To whom correspondence should be addressed. Tel: +49 331 977 2810; Fax: +49 331 977 2512; Email: bmr@uni-potsdam.de

customized synTALE-DBDs, which specifically target any plasmid-born or genome located promoter region upstream of the gene of interest (GOI).

Phytochromobilin (P $\Phi$ B), the chromophore of PhyB, is naturally not available in yeast. Therefore, phycocyanobilin (PCB), a P $\Phi$ B analog that can serve as a cofactor of PhyB, needs to be supplied exogenously (24–26). To overcome this, we engineered yeast to produce both chromophores in sufficient amounts. Comparable approaches have already been reported in bacteria, mammalian cells and *Pichia pastoris*, but not in *S. cerevisiae* (27–30). With this, we guarantee a nearly gratuitous gene induction system, making it potentially useful, even for large-scale applications.

We established two versions of the PhiReX system enabling either the tight control of gene expression with low basal expression levels and moderate expression output or slightly elevated background expression with high expression output, comparable to the strong yeast *TDH3* promoter. As PhiReX is compatible with the previously reported multi-gene assembly strategy AssemblX (31) it represents a perfect tool for pathway engineering.

## MATERIALS AND METHODS

### Strains, growth conditions and reagents

*Escherichia coli* strains DH5 $\alpha$  as well as NEB5 $\alpha$  and NEB10 $\beta$  (New England Biolabs, Frankfurt am Main, Germany) were employed for DNA cloning. Cells were grown at 37°C and 230 rpm in Luria-Bertani (LB) medium, with kanamycin or ampicillin (50 mg/ml) as selection marker. For yeast experiments, *S. cerevisiae* strain YPH500 (ATCC 76626) was cultured at 30°C and 230 rpm in Yeast extract Peptone Dextrose Adenine (YPDA)-rich medium or in appropriate Synthetic Dextrose (SD) media for selection of transformed cells.

### Constructs, DNA assembly and cell transformation protocols

Plasmid pLOGI, used as template for PCR amplification of the reporter gene yEGFP, was a gift from Tom Ellis, Imperial College London (32). Plasmids p414-TEF1p-Cas9-CYC1t and p426-SNR52p-gRNA.CAN1.Y-SUP4t were gifts from George Church (Addgene plasmids # 43802 and 43803). pMLM3705 was a gift from Keith Joung (Addgene plasmid # 47754) (33). All other plasmids reported in this study were established using AssemblX (31) in combination with the overlap-based DNA assembly methods SLiCE (34), Gibson assembly (35), NEBuilder HiFi DNA Assembly (New England Biolabs, Frankfurt am Main, Germany) and TAR (36). *In vitro* overlap-based cloning methods were used as previously reported (34,35). To this end, DNA fragments harboring 25- to 36-bp long homology regions were produced by PCR and assembled with linearized and dephosphorylated plasmids. *Escherichia coli* transformations were performed according to the High Efficiency Transformation Protocol from New England Biolabs. The correctness of DNA assemblies was verified by sequence analysis (LGC Genomics, Berlin, Germany). For *in vivo* DNA assembly, *S. cerevisiae* transformations were carried out following the LiAc/SS carrier DNA/PEG method by Gietz

and Schiestl (37). Information about all yeast strains obtained in this study is provided in Table 1. The AssemblX toolkit enables level-based multi-gene assemblies (31). While Level 0 plasmids are generally employed to assemble transcriptional units (TUs), Level 1 vectors allow the combination of up to five Level 0 modules. AssemblX was used in a preliminary version with vector backbones and homology regions slightly different from the final version (sequences available in Supplementary Data File 1). Supplementary Table S1 lists all parts used in this study with appropriate sources and, if applicable, sequence modifications. Sequences of all constructs described here are given in Supplementary Data File 1. Sequences of oligonucleotides are available in Supplementary Table S2.

### Generation of Level 0 and Level 1 constructs containing the light-inducible split synTF

For the construction of each multi-gene containing Level 1 plasmid, three appropriate Level 0 vectors (A1, A2 and A3) were constructed. Each Level 0 vector obtains homology regions for recombination with the Level 1 vector backbone or the neighboring Level 0 fragment. Each Level 1 vector contains three cassettes: (i) the synTALE-DBD-PhyB fusion, (ii) the PIF3-AD fusion, (iii) the reporter cassette, containing the reporter gene yEGFP, located downstream of a synthetic promoter, which consists of the synTALE-DBS and a *Cyc1* minimal promoter. Multi-gene containing Level 1 constructs were generated by combining three Level 0 fragments, released from the preassembled AssemblX Level 0 constructs A1, A2 and A3 with the Level 1 vector backbone pL1A\_Leu\_Lc, a CEN/ARS plasmid with selection marker *LEU2* and homology regions A0 and B0. The different Level 1 plasmids and the appropriate Level 0 fragments are given in Supplementary Table S3.

For Level 0 plasmid pL0\_RL\_A1, the CDS for *PIF3*, the NLS of the simian virus 40 (SV40-NLS), and a quadruple tandem repeat of the herpes simplex virus VP16-AD (VP64-AD) were cloned as a fusion transcript under control of the strong constitutive yeast *FBA1* promoter and terminator into the AssemblX Level 0 A1 vector backbone pL0\_A0-A1. For construct pL0\_RL\_A2\_CT the CDS for PhyBNT (aa 1–621 of PhyB), the yeast *Cdc1*-NLS and the empty synTALE-backbone without RVD region, and for construct pL0\_RL\_A2\_NT the synTALE-backbone, *Cdc1*-NLS and PhyBNT were cloned as fusion transcripts in the indicated order under control of the *TDH3* promoter and terminator into the AssemblX Level 0 A2 plasmid pL0\_A1-A2. Syn-TALE1-RVD region was assembled to target sequence *Jub1.1* (TCTATAA-GATCTTGTGTGC, a region of the *JUB1* promoter from *Arabidopsis thaliana*; AGI code: At2g43000) following the protocol described in Morbitzer *et al.* (38), and subcloned as a BamHI and AgeI fragment into equally digested plasmids pL0\_RL\_A2\_CT and pL0\_RL\_A2\_NT, resulting in constructs pL0\_RL\_A2\_CT\_TALE and pL0\_RL\_A2\_NT\_TALE, respectively. For vector pL0\_RL\_A3 the synTALE-DBS-containing four repeats of *Jub1.1* were cloned upstream of the *Cyc1* minimal promoter. The CDS of yEGFP and the *Cyc1* terminator were cloned downstream of the resulting synthetic pro-

**Table 1.** Complete list of strains generated. All yeast strains were generated from YPH500 cells

Yeast strain	Genomic integration/ locus	Episomal plasmid	Selection
RL_CT	—	pRL_CT	Leu
RL_CT_w/o_DBS	—	pRL_CT_w/o_DBS	Leu
RL_CT_ADH1p	—	pRL_CT_ADH1p	Leu
RL_NT	—	pRL_NT	
RL_NT_w/o_DBS	—	pRL_NT_w/o_DBS	
RL_NT_ADH1p	—	pRL_NT_ADH1p	
RL_CT_GI	pRL_CT_GI/ <i>ura3-52</i>	pRL_yEGFP_hc	Leu/Ura
RL_CT_GI_w/o_DBS	pRL_CT_GI/ <i>ura3-52</i>	pRL_yEGFP_w/o_DBS_hc	Leu/Ura
RL_CT_GI_ADH1p	pRL_CT_GI/ <i>ura3-52</i>	pRL_yEGFP_ADH1p_hc	Leu/Ura
RL_GI_PCB27	pRL_CT_GI/ <i>ura3-52</i> pRL_GI_PCB27/ <i>his1-Δ200</i>	pRL_yEGFP_hc	Leu/Ura/Trp
RL_GI_PCB28	pRL_CT_GI/ <i>ura3-52</i> pRL_GI_PCB28/ <i>his1-Δ200</i>	pRL_yEGFP_hc	Leu/Ura/Trp
RL_GI_PCB29	pRL_CT_GI/ <i>ura3-52</i> pRL_GI_PCB29/ <i>his1-Δ200</i>	pRL_yEGFP_hc	Leu/Ura/Trp
RL_GI_PCB30	pRL_CT_GI/ <i>ura3-52</i> pRL_GI_PCB30/ <i>his1-Δ200</i>	pRL_yEGFP_hc	Leu/Ura/Trp
RL_GI_PCB31	pRL_CT_GI/ <i>ura3-52</i> pRL_GI_PCB31/ <i>his1-Δ200</i>	pRL_yEGFP_hc	Leu/Ura/Trp
RL_GI_PCB32	pRL_CT_GI/ <i>ura3-52</i> pRL_GI_PCB32/ <i>his1-Δ200</i>	pRL_yEGFP_hc	Leu/Ura/Trp
RL_GI_PCB33	pRL_CT_GI/ <i>ura3-52</i> pRL_GI_PCB33/ <i>his1-Δ200</i>	pRL_yEGFP_hc	Leu/Ura/Trp
RL_GI_PCB34	pRL_CT_GI/ <i>ura3-52</i> pRL_GI_PCB34/ <i>his1-Δ200</i>	pRL_yEGFP_hc	Leu/Ura/Trp
RL_CT_w/o_PhyBNT_w/o_PIF3-AD	—	pRL_CT_w/o_PhyBNT_w/o_PIF3-AD	Leu
RL_CT_w/o_PIF3-AD	—	pRL_CT_w/o_PIF3-AD	Leu
RL_CT_w/o_TALE	—	pRL_CT_w/o_TALE	Leu
RL_CT_GI.del1 = PhiReX 1.0	pRL_CT_GI.del1/ <i>ura3-52</i>	pRL_yEGFP_hc	Leu/Ura
RL_CT_GI.del2	pRL_CT_GI.del2/ <i>ura3-52</i>	pRL_yEGFP_hc	Leu/Ura
RL_CT_GI.del1.1	pRL_CT_GI.del1.1/ <i>ura3-52</i>	pRL_yEGFP_hc	Leu/Ura
RL_CT_GI.del2.1	pRL_CT_GI.del2.1/ <i>ura3-52</i>	pRL_yEGFP_hc	Leu/Ura
RL_CT_GI.del1.2 = PhiReX 1.1	RL_CT_GI.del1.2*/ <i>ura3-52</i>	pRL_yEGFP_hc	Leu/Ura
RL_CT_GI.del2.2	RL_CT_GI.del2.2*/ <i>ura3-52</i>	pRL_yEGFP_hc	Leu/Ura
RL_CT_GI.del1.3	RL_CT_GI.del1.3*/ <i>ura3-52</i>	pRL_yEGFP_hc	Leu/Ura
RL_CT_GI.del1.4	RL_CT_GI.del1.4*/ <i>ura3-52</i>	pRL_yEGFP_hc	Leu/Ura
RL_CT_GI.del1.5	RL_CT_GI.del1.5*/ <i>ura3-52</i>	pRL_yEGFP_hc	Leu/Ura
RL_CT_GI.del2.5	RL_CT_GI.del2.5*/ <i>ura3-52</i>	pRL_yEGFP_hc	Leu/Ura
RL_CT_GI.del2.6	RL_CT_GI.del2.6*/ <i>ura3-52</i>	pRL_yEGFP_hc	Leu/Ura
PhiReX 1.0+	pRL_CT_GI.del1/ <i>ura3-52</i> pRL_GI_PCB28/ <i>his1-Δ200</i>	pRL_yeGFP_hc	Leu/Ura/Trp

moter into the AssemblX Level 0 A3 plasmid pL0\_A2-AR. Plasmid pL0\_RL\_A3\_w/o\_DBS was cloned by inserting a stuffer sequence instead of the synTALE-DBS. Plasmid pL0\_RL\_A3\_ADH1p was cloned by inserting the *ADH1* promoter instead of the synTALE-DBS and the *Cyc1* minimal promoter with overlap based cloning methods.

#### Generation of constructs required for the genome integration of the red light-inducible split synTF

For genome integration of the red light-inducible split synTF, Level 0 fragments were released from Level 0 vectors pL0\_RL\_A1 and pL0\_RL\_A2\_CT.TALE and cloned together with the *LEU2* selection marker into plasmid pFM75, resulting in plasmid pRL\_CT\_GI. Plasmid pFM75 is designed for genome integration into the *ura3-52* locus of the yeast genome, after PmeI digestion. The reporter cassette remained on plasmid. For this, Level 0 fragments pL0\_RL\_A3, pL0\_RL\_A3\_w/o\_DBS and pL0\_RL\_A3\_ADH1p were released from their backbones and cloned into pL0\_A2-A3\_Ura, a Level 0 vector with 2-micron origin and selection marker *URA3*, resulting in

plasmids pRL\_yEGFP\_hc, pRL\_yEGFP\_ADH1p\_hc and pRL\_yEGFP\_w/o\_DBS\_hc.

#### Generation of constructs for minimization of basal expression levels

To investigate reasons for the high basal expression levels of pRL\_NT and pRL\_CT, Level 1 constructs pRL\_CT\_w/o\_TALE, pRL\_CT\_w/o\_PhyBNT\_w/o\_PIF3-AD and pRL\_CT\_w/o\_PIF3-AD were constructed. For this, Level 0 plasmids pL0\_RL\_A2.TALE\_w/o\_PhyB and pL0\_RL\_A2\_CT\_w/o\_TALE were cloned. For construction of pL0\_RL\_A2.TALE\_w/o\_PhyB the yeast Cdc1-NLS and the synTALE-backbone were cloned as fusion transcript under control of the *TDH3* promoter and *TDH3* terminator into the AssemblX Level 0 A2 vector backbone pL0\_A1-A2. SynTALE1 and plasmid pL0\_A1-A2 were digested with restriction endonucleases BamHI and AgeI and the released synTALE-repeats were cloned into the linearized backbone. For pL0\_RL\_A2\_CT\_w/o\_TALE the Cdc1-NLS and the CDS of PhyBNT were cloned under control of the *TDH3* promoter and *TDH3* terminator into the AssemblX Level 0 A2 plasmid pL0\_A1-A2. Level 1 constructs were generated

by combining Level 0 fragments, released from the different AssemblX Level 0 constructs A1, A2 and A3, and Level 1 vector backbone pL1A\_Leu\_lc, as described in Supplementary Table S3.

To lower the basal expression levels of pRL\_CT\_GI, the Cdc1-NLS incorporated in the PhyB-synTALE fusion and also the NLS sequences present in the synTALE-backbone were deleted. For this, plasmids pRL\_CT\_GI.del1 and pRL\_CT\_GI.del2 were constructed (Supplementary Table S4). All primers used for mutagenesis are listed in Supplementary Table S2. For the construction of pRL\_CT\_GI.del1 a PCR product obtained with primers L772/L762 and template pL0\_RL\_A2\_CT\_TALE was inserted into SmaI/AatII-linearized pRL\_CT\_GI. To obtain construct pRL\_CT\_GI.del2, a PCR product obtained with primers L662/L767 and template pRL\_CT\_GI was inserted into AgeI-linearized Level 1 vector pRL\_CT\_GI. Furthermore, the nuclear export signal (NES) of the protein kinase inhibitor peptide (PKI) was added in between PhyBNT and the synTALE of plasmids pRL\_CT\_GI.del1 and del2, resulting in plasmids pRL\_CT\_GI.del1.1 and del2.1. For these constructs, PCR products obtained with primers L795/L796 and template pRL\_CT\_GI were inserted into BamHI/SacI-digested plasmids pRL\_CT\_GI.del1 and pRL\_CT\_GI.del2, respectively. For the construction of pRL\_CT\_GI.del2.2, which contains a PKI-NES at the C-terminal domain of the PhyBNT-synTALE fusion, a PCR product obtained with primers L767/L797 and template pRL\_CT\_GI was inserted into AgeI-digested plasmid pRL\_CT\_GI.del2.

Plasmids pRL\_CT\_GI.del1, pRL\_CT\_GI.del2, pRL\_CT\_GI.del1.1, pRL\_CT\_GI.del2.1 and pRL\_CT\_GI.del2.2 were genome integrated and cotransformed with the reporter construct pRL\_yeGFP\_hc to yield strains RL\_CT\_GI.del1/del2, RL\_CT\_GI.del1.1/del2.1 and strain RL\_CT\_GI.del2.2.

A Cas9-based genome editing approach was followed for the construction of additional variants of the strains, given in detail in Supplementary Table S4 and Figure 4B: (i) Addition of a PKI-NES to the C-terminus of the synTALE-PhyBNT fusion of strain RL\_CT\_GI.del1 to yield RL\_CT\_GI.del1.2\*. (ii) Addition of a Cdc1-NLS to the N-terminus of the PIF3-SV40-NLS-AD fusion of strain RL\_CT\_GI.del1 to obtain RL\_CT\_GI.del1.3\*. (iii) Deletion of the SV40-NLS of the PIF3-AD fusion of strain RL\_CT\_GI.del1 to yield strain RL\_CT\_GI.del1.4\*. (iv) Addition of a Cdc1-NLS to the N-terminus of the PIF3-SV40-NLS-AD fusion of strains RL\_CT\_GI.del1.2\* and RL\_CT\_GI.del2.2\* to obtain RL\_CT\_GI.del1.5\* and RL\_CT\_GI.del2.5\*. (v) Deletion of the SV40-NLS of strain RL\_CT\_GI.del2.2\* to yield RL\_CT\_GI.del2.6\*.

Shortly described, respective yeast cells, given in Supplementary Table S4, were transformed with the Cas9 expression plasmid p414-TEF1p-Cas9-CYC1t (39), the appropriate sgRNA expression plasmid and the donor DNA as a repair template. To generate sgRNA cloning and expression plasmid pFM21, we modified plasmid p426-SNR52p-gRNA.CAN1.Y-SUP4t (39) by exchanging the *URA3* marker for the *LEU2* marker gene and by introducing a BamHI-EcoRI cloning site between the structural sgRNA backbone and the *SNR52* pro-

moter. Individual sgRNA expression cassettes were generated via NEBuilder HiFi DNA Assembly (New England Biolabs) of double-stranded oligonucleotides into pFM21. As previously described, the donor DNA was generated from two overlapping oligonucleotides (40). Oligonucleotides used for sgRNA cloning and sgRNA sequences are given in Supplementary Tables S2 and S4. Strains RL\_CT\_GI.del1.2\*/3\*/4\*/5\* and RL\_CT\_GI.del2.5\*/6\* were cotransformed with the reporter construct pRL\_yeGFP\_hc to yield strains RL\_CT\_GI.del1.2/3/4/5 and RL\_CT\_GI.del2.5/6. Details about the generated strains are given in Table 1.

### Generation of constructs for chromophore biosynthesis in yeast

Two enzymes are required for the production of the PhyB chromophores PCB and PΦB: a heme oxygenase (HO) and a bilin reductase (BR). Different combinations of native and modified sequences of HOs, i.e., *HY1* from *A. thaliana* and *Hmx1* from *S. cerevisiae*, and BRs, i.e. *HY2* from *A. thaliana* and *PcyA* from *Synechocystis sp.*, were tested. Details are given in Supplementary Table S1. HOs were set under control of the yeast *PGK1* promoter and terminator and cloned into linearized Level 0 vector pL0\_A3-A4 resulting in Level 0 plasmids pPCB1, pPCB2, pPCB3 and pPCB4. BRs were cloned under control of the yeast *ADH1m* promoter and the *ADH1* terminator and cloned into linearized AssemblX Level 0 vector backbone pL0\_A4-HR\_ADH1t, resulting in Level 0 constructs pPCB5b, pPCB6b, pPCB7b and pPCB8b. For the construction of plasmids pRL\_GI\_PCB\_27 to pRL\_GI\_PCB\_34, different combinations of Level 0 vectors, given in Supplementary Table S3, were inserted into linearized vector backbone pRL\_GI\_PCB1. Plasmid pRL\_GI\_PCB1 allows genome integration of Level 1 cassettes into the *his1-Δ200* locus after release of the Level 1 cassette by restriction with PmeI or SbfI, respectively.

### Generation of plasmid pYES2CT\_yEGFP and expression experiments

In order to compare PhiReX 1.0+ with the well-established, galactose-inducible *GAL1* promoter, the commercially available expression vector pYES2/CT (Thermo Fisher Scientific, Waltham, MA, USA) was digested with HindIII and PmeI and the CDS of the reporter gene yEGFP was cloned in between the two recognition sites to yield plasmid pYES2/CT\_yEGFP. Galactose induction was done according to the Invitrogen user manual for part no. 25-0304 (Rev. date: 30 November 2009). Precultures and uninduced samples were maintained in glucose containing medium.

### PCR methods

PCR amplifications were done using either Q5 DNA polymerase (New England Biolabs) or Phusion polymerase (Life Technologies, Darmstadt, Germany), according to the manufacturer's instructions.

### Light induction experiments

If not mentioned otherwise, cells were inoculated in 1 ml appropriate SD-medium, containing 2% glucose, and incubated for 24 h at 30°C and 230 rpm in 12-well cell culture plates (TPP Techno Plastic Products AG, Trasadingen, Switzerland; order number 92412). Cultures were immediately irradiated with a 30-sec far-red light pulse and grown for 6 h at 30°C and 230 rpm in the dark. Thereafter, induced cells were treated with a 30-sec red light pulse, followed by 10-sec red light pulses every 30 min over a period of 16 h, while uninduced cells were maintained in darkness. Protein production was stopped by adding 50  $\mu$ l 10 mg/ml cycloheximide. Fluorescence output of single cells was measured by flow cytometry as described before (31). If not stated differently, the presented results are mean values calculated from three biologically independent measurements, each with three technical replicates. Standard deviation is indicated by error bars.

### Light sources

LED light sources for red light ( $\lambda = 640\text{--}680$  nm, peak at 661 nm) and far-red light ( $\lambda = 720\text{--}760$  nm, peak at 740 nm) were installed by COMPLED Solutions GmbH (Dresden, Germany) into an INFORS HT Multitron Pro (INFORS, Bottmingen, Switzerland). For each wavelength, 40 LEDs were placed at the inner ceiling of the incubator. Light-reflecting foil was installed on the walls to ensure even illumination at a light intensity of 2.8 mW/cm<sup>2</sup> for red light, and 6.9 mW/cm<sup>2</sup> for far-red light. All light-sensitive manipulations were done in a dark room under green safelight using a standard LED strip.

## RESULTS

### Establishment of a red light-induced split synTF

The PhiReX system described here is a red/far-red light-dependent expression system based on two fusion proteins: a synTALE-DBD linked to an N-terminal version of the light-sensitive photoreceptor PhyB (PhyBNT) and a fusion of the PhyB interacting partner PIF3 with the VP64-AD (Figure 1A). The synTALE-DBD was programmed to specifically target the synTALE-DBS located upstream of a minimal promoter and the reporter gene *yEGFP*. The synTALE-PhyBNT fusion protein binds the synTALE-DBS, regardless of the light condition (Figure 1B). However, dimerization with the PIF3-AD fusion protein and subsequent activation of gene expression are red light-induced. We designed two multi-gene CEN/ARS plasmids, pRL<sub>NT</sub> and pRL<sub>CT</sub>, which differ with respect to the PhyBNT-synTALE fusion: the synTALE-DBD was fused to the N-terminus (NT) or C-terminus (CT) of PhyBNT, respectively, whereby Cdc1-NLS links the two components (Figure 1A).

As the natural chromophore of the plant photoreceptor PhyB, P $\phi$ B, is not synthesized in yeast, the analogous compound PCB which can act as a chromophore of PhyB was supplied to the medium (24,25). To show PCB-dependent and red light-specific activation of protein expression, we measured yEGFP fluorescence of RL<sub>NT</sub> and RL<sub>CT</sub> cells

grown in the dark or treated with red light pulses in drop-out medium containing different PCB concentrations (0–50  $\mu$ M). For both cell types, we observed growing red light-mediated yEGFP output with increasing PCB concentrations, reaching a plateau at concentrations of 25  $\mu$ M (Figure 2). All following experiments were therefore carried out with media containing 25  $\mu$ M PCB. A very low yEGFP signal was observed for the negative controls lacking the synTALE-DBS. The absolute values of yEGFP fluorescence and the fold induction ( $\sim 3.3$ -fold with 25  $\mu$ M PCB) were similar in RL<sub>NT</sub> and RL<sub>CT</sub> cells. However, RL<sub>NT</sub> showed no light-induced yEGFP fluorescence in the absence of PCB, while RL<sub>CT</sub> exhibited red light-dependent yEGFP signal (fold induction  $\sim 2.4$ ) (Figure 2). This observation is consistent with a phytochrome A (PhyA)-based system previously reported, which also showed red light-triggered expression without exogenous supply of chromophore in *S. cerevisiae*, suggesting that an unidentified cellular metabolite functions as a chromophore for the photoreceptor (16). As light induction in the absence of exogenous chromophore was only observed for RL<sub>CT</sub>, this system may be more sensitive than RL<sub>NT</sub> and was therefore used for further experiments.

### Combining genome integrated regulators and an episomal reporter cassette results in boosted fluorescence output upon red light induction

To achieve stable and robust protein expression, we integrated the C-terminal version of the PhyBNT-synTALE fusion and PIF3-AD into the *ura3–52* locus of the yeast genome. The expression cassette, containing the target promoter and the reporter, remained on a plasmid to enable an easy and flexible exchange of the GOI (Figure 3A). To design a system generating high expression output, a high-copy 2-micron origin of replication was selected for the reporter construct, as opposed to plasmid pRL<sub>CT</sub>, which harbors the low-copy CEN/ARS replication origin. This optimized system, RL<sub>CT</sub>\_GI, yields a reliable induction in usually more than 80% of cells. In comparison, the percentage of activated cells in RL<sub>CT</sub> varied between less than 10% to much higher values reaching 80%. yEGFP fluorescence obtained for RL<sub>CT</sub>\_GI was 55-fold higher (fold induction  $\sim 6.3$ ), compared to RL<sub>CT</sub> (fold induction  $\sim 3.9$ ) (Figure 3B). However, also basal expression levels increased strongly. As RL<sub>CT</sub>\_GI<sub>ADH1p</sub> and RL<sub>CT</sub>\_GI<sub>w/o\_DBS</sub> (Table 1) show an obvious increase as well, the boost of reporter output is most likely due to the generally higher expression output from high-copy plasmids.

### Improving fold induction by minimizing basal expression levels

The high basal expression levels observed for RL<sub>CT</sub>\_GI may be due to different reasons, including e.g. the following: yeast endogenous TFs binding to the synTALE-DBS, thereby activating gene expression; a cryptic DBD in the PIF3-AD fusion, that binds to the synTALE-DBS; unspecific interaction between the PIF3-AD and PhyBNT-synTALE fusions, activating transcription independent of

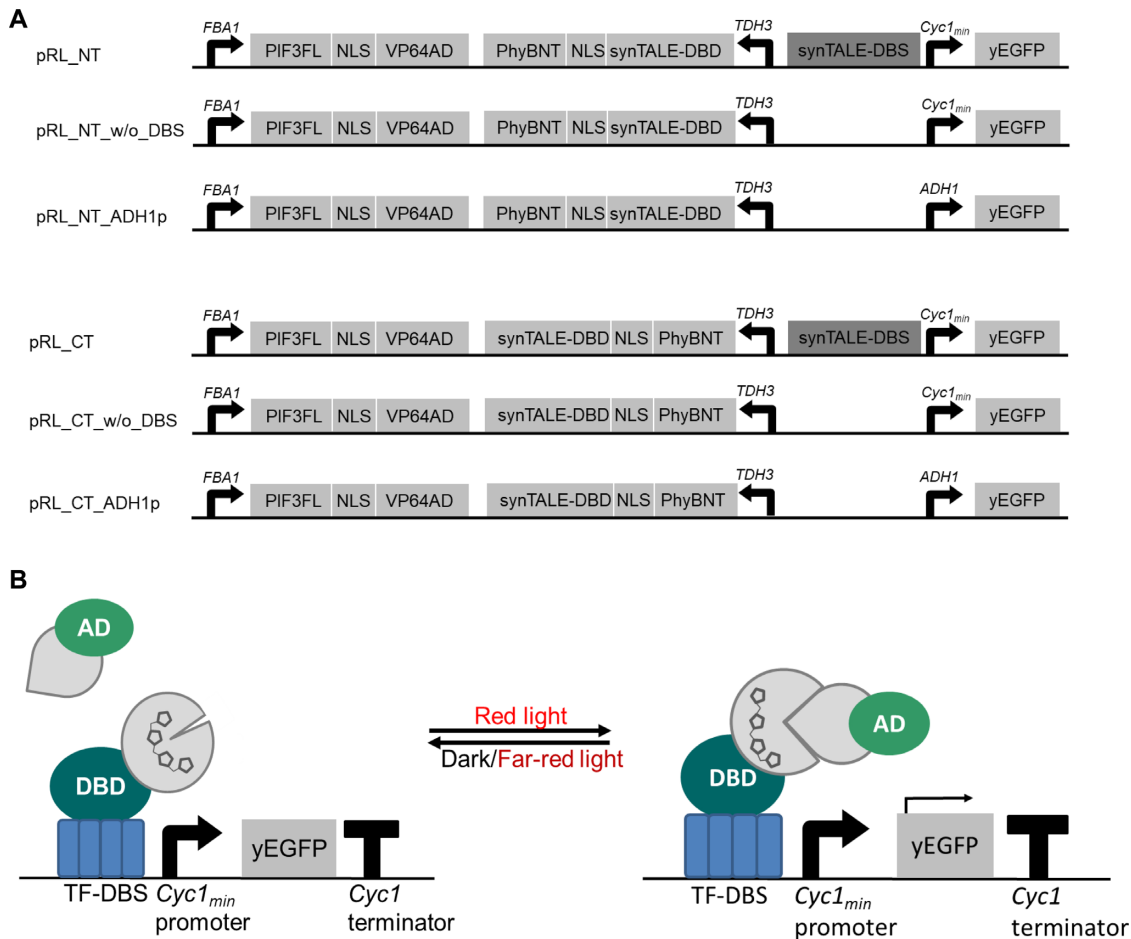


**Figure 1.** Schematic overview and design of the PhiReX-system. (A) Design of light-responsive constructs pRL\_NT and pRL\_CT, negative control plasmids lacking the synTALE-DBS (pRL\_NT\_w/o\_DBS and pRL\_CT\_w/o\_DBS), and plasmids with *yEGFP* under control of the constitutive yeast *ADHI* promoter as a technical control (pRL\_CT\_ADHIp and pRL\_NT\_ADHIp). (B) Mode of action of pRL\_NT and pRL\_CT. In the dark or in far-red light ( $\lambda = 740$  nm) the PhyB-synTALE-DBD fusion binds to its DBS. Stimulation with red light ( $\lambda = 660$  nm) induces dimerization of the split transcription factor leading to activation of *yEGFP* expression.

light conditions; intrinsic ADs in the synTALE-PhyB fusion that activate transcription in a light-independent manner. To determine the actual cause of (high) basal expression levels, different plasmids were constructed and tested with regard to *yEGFP* fluorescence (Supplementary Figure S1 and Supplementary Table S3). Our results show that the synTALE-DBD fusion is largely responsible for the high *yEGFP* levels observed in the uninduced state. However, basal expression levels of RL\_CT are higher than those containing solely the synTALE-DBD or the PhyBNT-synTALE fusion. This leads to the interpretation that unspecific and light-independent interaction of PhyBNT with PIF3, which cannot be reliably tested, causes an additional effect, as all other reasons can be excluded considering the results obtained in this experiment.

To lower the synTALE-mediated background activity, we modified PhyBNT-synTALE to prevent translocation of the protein to the nucleus before red light irradiation. Upon light application, interaction of PhyB-synTALE with the NLS-containing PIF3-AD fusion allows translocation of the protein complex to the nucleus and concomitant activation of gene expression. To this end, the following mod-

ifications were introduced to the optical dimerizer (Figure 4, Supplementary Table S4): (i) Deletion of the Cdc1-NLS from the PhyBNT-synTALE fusion. (ii) Deletion of previously reported internal NLS sequences in the synTALE to prevent nuclear localization before induction (41) (Figure 4A). (iii) Addition of a nuclear export signal (NES) to the PhyBNT-synTALE fusion, to localize the protein to the cytoplasm (Figure 4B). (iv) Insertion of an additional Cdc1-NLS to the PIF3-SV40NLS-AD fusion to support efficient nuclear import of the large complex consisting of the PhyB-synTALE and the PIF3-AD fusions. (v) Deletion of the SV40-NLS from the PIF3-AD fusion to allow undisturbed native interaction between PhyB and PIF3 resulting in nuclear import of the dimerized fusion protein only after light application (42–44). The various constructs were analyzed for red light-induced reporter gene expression (Supplementary Figure S2). The best results considering basal expression levels and fold induction were observed for RL\_CT\_GI.del1 lacking all potential NLS sequences in the PhyB-synTALE fusion (PhiReX 1.0) and RL\_CT\_GI.del1.2 (PhiReX 1.1) containing an additional PKI-NES in the PhyB-synTALE fusion (Figure 4B and C).

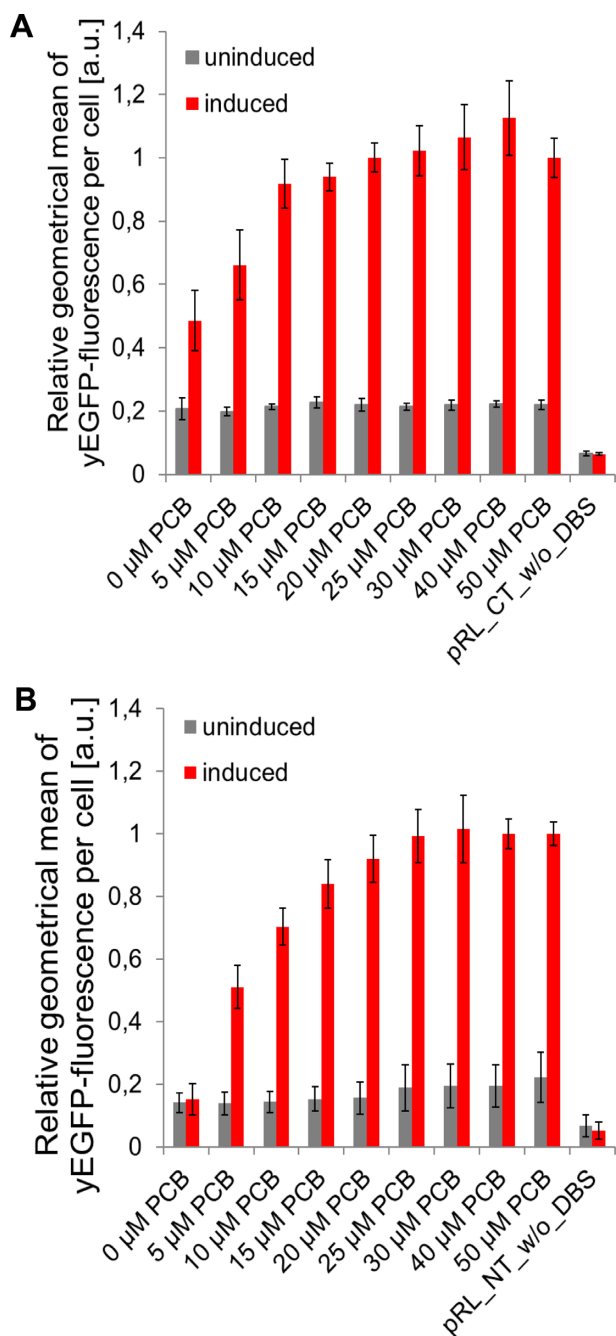


**Figure 2.** PCB-dependent yEGFP output of the red light-sensing expression systems. (A) RL\_CT and (B) RL\_NT yeast cells were grown in SD-Leu medium with 0–50  $\mu\text{M}$  PCB for 6 h in darkness. Induced cells were treated with 10-sec red light pulses every 30 min for 16 h. Uninduced cells remained in the dark. Yeast cells RL\_NT\_w/o\_DBS and RL\_CT\_w/o\_DBS were grown in SD-Leu medium with 25  $\mu\text{M}$  PCB. Output of yEGFP was measured via flow cytometry. a.u.: arbitrary units.

In medium containing 25  $\mu\text{M}$  PCB, PhiReX 1.0 confers 11-fold induction and high expression output, similar to the strong yeast *TDH3* promoter. PhiReX 1.1 shows nearly no background activity and high fold induction of up to 41. The expression levels upon light induction are comparable to those of the medium strong yeast *ADH1* promoter.

## Engineering yeast to produce the chromophores PCB and P $\Phi$ B

Even though RL\_CT\_GI shows low red light-mediated reporter expression in the absence of PCB, we proposed that expression output can be increased by engineering a yeast strain that endogenously produces the chromophores PCB or P $\Phi$ B from the precursor heme naturally present in the host. To achieve this, two enzymes are required: a heme oxygenase (HO) which catalyzes the conversion of heme to biliverdin, and a bilin reductase (BR) which converts biliverdin further to P $\Phi$ B or PCB, depending on the source organism (Figure 5A) (27). We designed and tested different combinations of native and modified HOs and BRs derived from *A. thaliana* (*HY1*, *HY2*), *Synechocystis* sp. (*PcyA*) and *S. cerevisiae* (*Hmx1*) (Figure 5B). The different expression cassettes were genome integrated into the *his1- $\Delta$ 200* locus of RL\_CT\_GI cells (Figure 5C). Previous studies in mammalian cells (28) and *Pichia pastoris* (29) revealed optimized chromophore biosynthesis when the two biosynthesis enzymes were targeted to mitochondria, the location of heme biosynthesis in eukaryotes (45). Accordingly, we deleted the proteins' native target sequences, if applicable, and replaced them by a yeast-derived mitochondrial targeting sequence (MTS) (Supplementary Table S1). As reporter output depends on chromophore concentration (Figure 2), the most efficient enzyme combination for holo-phytochrome production was determined by measuring yEGFP fluorescence of RL\_GI\_PCB27–34 in the absence of exogenous PCB. All combinations showed increased expression levels compared to RL\_CT\_GI, with the highest values observed for RL\_GI\_PCB28 (*HY1*, *PcyA*), RL\_GI\_PCB31 (MTS-*mHY1*, MTS-*mHY2*), RL\_GI\_PCB32 (MTS-*mHY1*, MTS-*PcyA*), and RL\_GI\_PCB33 (MTS-*mHmx1*, MTS-*mHY2*), reaching approximately 3.5-fold induction in all combinations (Figure 5D). As the red light-mediated fold induction was distinctly higher in cells harboring genome integrated chromophore biosynthesis genes than in cells lacking HO and BR, we concluded that yeast was successfully engineered to produce PCB and P $\Phi$ B regardless of the localization of the enzymes. The expression cassette of pRL\_GI\_PCB28 for endogenous chromophore production was genome integrated into PhiReX 1.0, to yield strain PhiReX 1.0+, which is independent of chromophore supply.

## Characterization of PhiReX

In a time-course experiment, PCB producing PhiReX 1.0+ was analyzed in comparison to the strong constitutive yeast *TDH3* promoter and the galactose-inducible *GALI* promoter (Figure 6A). Our results demonstrate that PhiReX 1.0+ mediates a robust expression already 4 h after light induction, with expression levels reaching those of the *TDH3* promoter after 8 h. The reporter output is stable for at least 48 h. The achieved fold induction is comparable to that of the *GALI* promoter, while PhiReX 1.0+ mediates a much higher expression output; basal expression levels of PhiReX 1.0+ exceed those of the *GALI* promoter. Notably, the PhiReX 1.1 system described above confers very

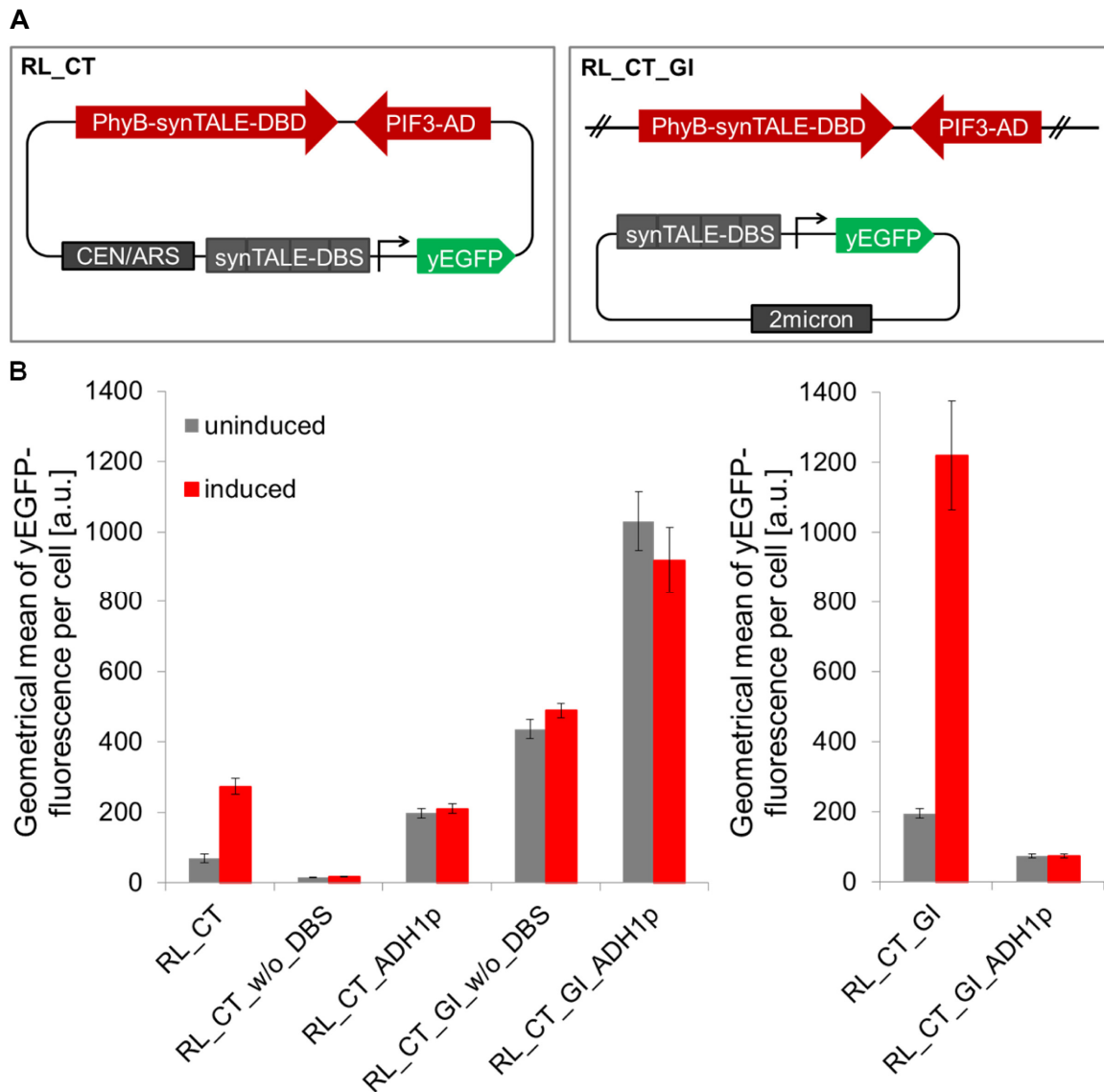


**Figure 3.** Comparison of red light-induced yEGFP fluorescence of yeast cells RL\_CT and RL\_CT\_GI. (A) Schematic overview of RL\_CT and RL\_CT\_GI showing the difference of the episomal (RL\_CT) and genome integrated system (RL\_CT\_GI). In the episomal system, all three parts are located on one CEN/ARS plasmid. For the genome integrated system, only the reporter cassette is located on a 2-micron plasmid while the PhyB-synTALE and the PIF3-AD fusions were genome integrated. (B) Measurement of light-induced gene expression to compare RL\_CT and RL\_CT\_GI. RL\_CT\_w/o\_DBS and RL\_CT\_GI\_w/o\_DBS served as negative controls without synTALE-DBS. RL\_CT\_ADH1p and RL\_CT\_GI\_ADH1p served as technical controls and enable comparison with the medium-strong yeast *ADH1* promoter. Yeast cells were grown in SD-Leu and SD-Leu-Ura selection media with 25  $\mu$ M PCB for 6 h in darkness. Induced cells were treated with a 30-sec red light pulse and grown for another 16 h with 10-sec red light pulses every 30 min. Uninduced cells remained in darkness. The left graph represents measurements with high detector sensitivity, while the right graph represents measurements with lower detector sensitivity. Detector sensitivity was modified due to strong yEGFP fluorescence achieved by RL\_CT\_GI. a.u.: arbitrary units.

low background activity and therefore is a suitable alternative for applications requiring reduced basal expression. To provide a reliable basis for researchers intending to work with PhiReX, we further showed that the PhiReX 1.0+ system exhibits light dose dependency and reversibility (Figure 6B and C): we applied single light pulses of various lengths and determined reporter output 4 h post-induction. Notably, a short light pulse of only five seconds is sufficient to induce reporter expression. A stepwise prolongation of the light pulse to up to 120 s results in increased yEGFP fluores-

cence. Thereby, PhiReX 1.0+ provides an easy way to fine-tune gene expression output. To test the reversibility of induction by red/far-red light application, PhiReX 1.0+ was treated with light pulses of different wavelength. While illumination with red light of 660 nm induced gene expression, far-red light (740 nm) reliably switched off protein production. Re-induction was readily achieved by a second round of red light application.

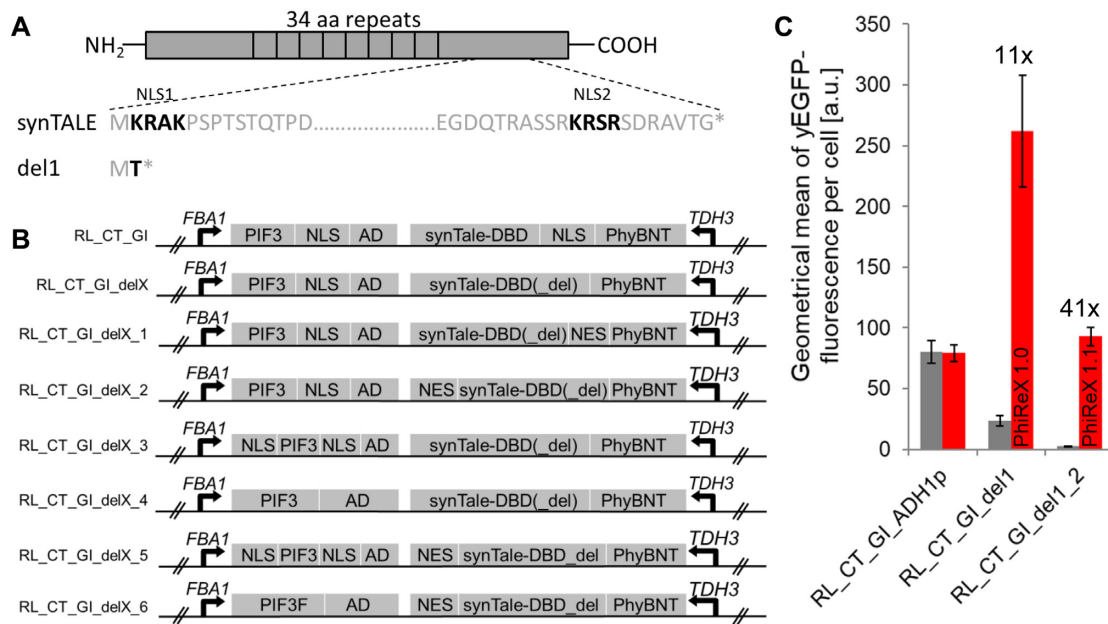


**Figure 4.** Strategy for minimizing basal expression levels. **(A)** Deletion of previously reported NLS sequences from the synTALE backbone. **(B)** Schematic overview of different RL\_CT.GI modifications. The NLS sequences present in the PhyB-synTALE fusion were deleted. In some cases, a single NES sequence was inserted at different positions, and NLS sequences were added to the PIF3-AD fusion. **(C)** Comparison of the two most promising versions, RL\_CT.GI.del1 and RL\_CT.GI.del1\_2, dubbed PhiReX 1.0 and PhiReX 1.1, respectively. Yeast cells were grown in SD-Ura-Leu medium with 25  $\mu$ M PCB for 6 h in darkness. Induced cells were treated with a 30-sec red light pulse, followed by 10-sec red light pulses every 30 min for 16 h. Uninduced cells and RL\_CT.GI.ADHIp cells remained in the dark. Output of yEGFP was measured via flow cytometry. Fold induction is indicated. a.u.: arbitrary units.

## DISCUSSION

The work presented here describes the development of a user-friendly, programmable, dose-dependent and robust red/far-red light-regulated gene expression switch, dubbed PhiReX, for application in the yeast *Saccharomyces cerevisiae*. Most important, PhiReX is independent of the supply of exogenous chromophore, making it perfectly suitable for large-scale production. PhiReX employs the N-terminal part of the photoreceptor PhyB (PhyBNT), which dimerizes with its interacting partner PIF3 in a red/far-red light dependent manner. The implementation of a synTALE-DBD allows its flexible programming to specifically target any DBS, synthetically generated or available in the host genome. Blue light-dependent regulation of gene expression, based on synTALE-DBDs, was previously reported for mammalian cells (46). However, to our knowledge no customizable light induction system has been developed for *S. cerevisiae* so far. The synTALE-mediated flexibility is a great advantage over DBDs with invariant binding specificity which limit the regulation to promoters harboring their native DBS; this is e.g. the case for GAL4-DBD, currently employed in several optogenetic expression systems (13–15). However, the synTALE-DBD (around 1,000 aa) is much larger than the GAL4-DBD (around 150 aa), which may hinder the conformational switch of the photoreceptor and the dimerization with PIF3. We therefore tested two different architectures of the PhyB-synTALE fusion where we linked the synTALE-DBD to either the N- or C-terminus of PhyBNT, resulting in plasmids pRL\_NT and pRL\_CT, respectively (Figure 1A). We found that both versions show comparable functionality regarding light- and

PCB-dependent reporter gene activation (Figure 2), with the only difference that RL\_CT induced yEGFP expression in red light also in the absence of supplied PCB. Red light activation without chromophore supply has already been reported in *S. cerevisiae*, indicating the presence of an unidentified cellular metabolite that functions as a chromophore (16). While in RL\_CT the N-terminal domain of PhyBNT is most likely freely accessible for chromophore attachment, binding of the unidentified chromophore may be hindered in RL\_NT (due to the presence of the large synTALE-DBD fused to the N-terminus of PhyBNT).

Although we were able to demonstrate light- and PCB-dependency for the initially developed light induction systems RL\_CT and RL\_NT, both showed great variability with respect to the number of activated cells and a high basal activity, indicating that further optimization was needed.

To achieve stable and robust expression, we integrated the PhyB-synTALE and the PIF3-AD fusions into the yeast genome. To enable an easy exchange of the GOI and to guarantee high expression levels, the reporter expression cassette was placed on a 2-micron high-copy plasmid. The first step of optimization yielded a great boost in yEGFP fluorescence output and a reliable and robust regulation of gene expression (Figure 3B).

Furthermore, we demonstrated that the high basal expression levels evident in the initial system result from the synTALE-DBD, which binds to the DBS irrespective of the light conditions (Supplementary Figure S1). Even though the TALE avrBS3 backbone harbors a single acidic AD at its C-terminus not included in the truncated synTALE-DBD employed here (47), an additional non-characterized

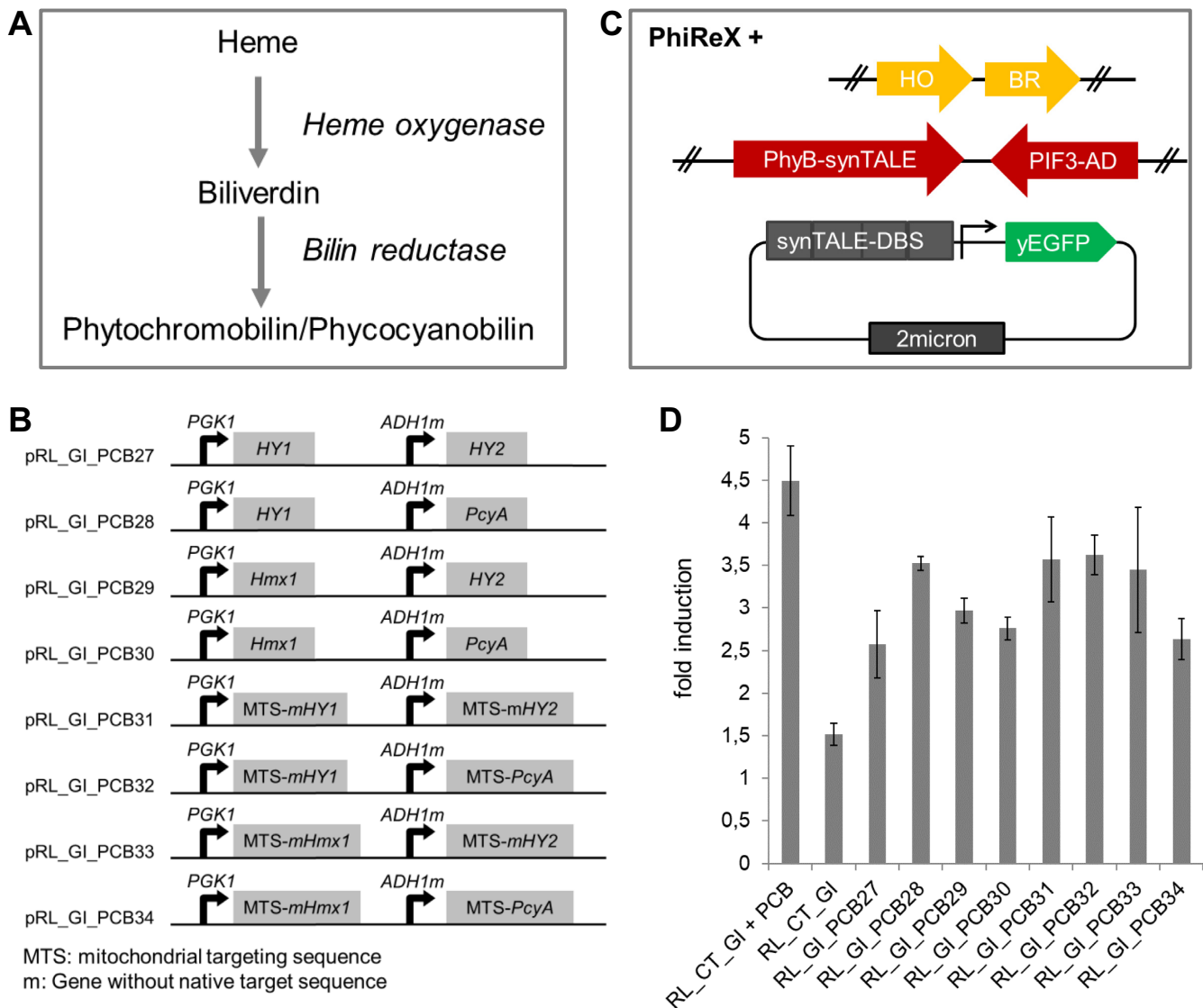


**Figure 5.** Chromophore biosynthesis in *S. cerevisiae*. (A) Overview of the conversion of heme to the chromophore via biliverdin. (B) Design of constructs pRL\_GI.PCB27–34, created to achieve PCB biosynthesis after genome integration into RL\_CT.GI. Heme oxygenases (HO) and bilin reductases (BR) from various organisms were constitutively expressed in different combinations. Native target sequences of HY1, HY2 and Hmx1 were deleted and mitochondrial targeting sequences were added to all proteins. (C) Scheme of the chromophore-independent PhiReX+ system. Red light-sensing synTF and chromophore biosynthesis components are genome integrated. The reporter construct is located on an episomal high-copy plasmid. (D) Fold induction of yEGFP output upon red light induction of RL\_CT.GI with PCB concentrations of 25  $\mu$ M (RL\_CT.GI + PCB) and 0  $\mu$ M (RL\_CT.GI) and of RL\_GI.PCB27–34 without PCB in the medium.

internal AD functional in *S. cerevisiae* may cause basal expression. Similarly, Konermann *et al.* reported high background levels for a synTALE-based blue light expression system in mammalian cells and suggested strategies to lower undesired expression by preventing nuclear localization of the synTALE-containing domain before light activation (46). Based on their results we redesigned our system to prevent nuclear import of the PhyB-synTALE fusion protein before dimerization with PIF3-AD which contains the strong SV40-NLS (Figure 4).

Therefore, the Cdc1-NLS included in the PhyB-synTALE fusion was deleted and potential NLS sequences in the synTALE backbone were mutated or deleted according to previous approaches (41). As PhyB contains NLS-like motifs

only in the C-terminus (48), there was no need to mutate or delete sequences in the PhyBNT photoreceptor used here. Furthermore, in plants PhyB is located in the cytoplasm and only enters the nucleus after dimerization with PIF3 (44). A similar behavior was observed in a cell-free system using isolated nuclei, and in mammalian cells (42,43). The PhyB-synTALE protein is thus expected to be located in the cytoplasm of yeast strain PhiReX 1.0 in the uninduced state, thereby preventing binding to its cognate DBS and activating target gene expression. PhiReX 1.0 showed reduced basal expression levels but high expression output in the induced state (comparable to the *TDH3* promoter), and a fold induction of up to 11 (Figure 4C). To further reduce leaky expression and exclude nuclear accumulation of

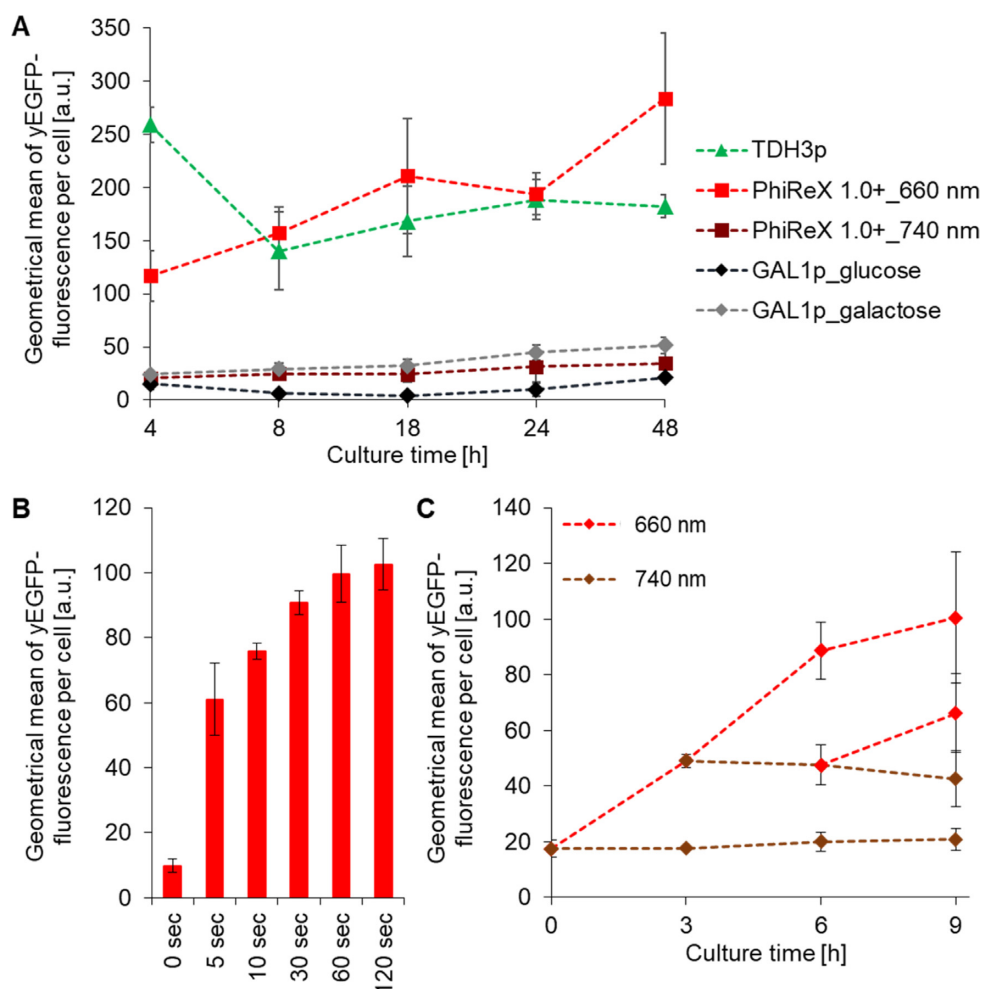


**Figure 6.** Characterization of PhiReX 1.0+. Yeast cells were grown in SD-Ura-Leu-Trp medium for 6 h in darkness prior to induction. (A) Time course of light-dependent reporter gene induction, compared to the constitutive *TDH3* promoter and the *GAL1* induction system (pYES2/CT). Cells were grown in a volume of 20 ml SD medium in 100-ml flasks. Output of yEGFP was measured via flow cytometry in a 48-h time course experiment. (B) Light dose dependency of PhiReX 1.0+ was measured by activating cells with a single light pulse of the indicated duration. Post-induction, cells were grown for 4 h in the dark and yEGFP was measured via flow cytometry for two biological replicates, each with three technical replicates. (C) Reversion of protein production via PhiReX 1.0+. Cells were grown in a volume of 20 ml SD medium in 100-ml flasks. Uninduced cells were grown in the dark, while induced cells were treated with a single 30-sec red light pulse, followed by 5-sec pulses every 30 sec. Reversion of gene expression was mediated by a 5-min far-red light pulse. Cultures were divided into two sub-cultures, of which one was treated with red light as indicated, while the other was further maintained in unchanged condition. yEGFP output was measured via flow cytometry for two biological replicates, each with three technical replicates. Line colors indicate light conditions of the respective samples: red lines indicate growth under inducing conditions; dark-red lines indicate growth in darkness after far-red light application. a.u.: arbitrary units.

PhyB-synTALE protein before interaction with PIF3-AD, we added the strong PKI-NES to the PhyBNT-synTALE fusion, resulting in PhiReX 1.1; this minimizes basal expression level and allows tight control of protein production with a fold induction of 41. Red light-mediated expression output of PhiReX 1.1 is comparable to that of the medium strong *ADHI* promoter. Due to its low background, this system is ideally suited for the expression of toxic proteins. Additional manipulations of the PIF3-AD fusion did not result in further improvements of the system (Figure 4B, Supplementary Figure S2).

The requirement for an exogenous supply of the chromophore PCB to support light-regulated gene expression devaluates the advantages of a light system as a cheap and easy-to-handle tool. Even though RL\_CT\_GI cells

show light-induced yEGFP output also in the absence of PCB, the obtained fold induction ( $\sim 1.5$ ) was not satisfying; this prompted us to engineer *S. cerevisiae* cells able to produce the chromophore by expressing the enzymes HO and BR which catalyze the conversion of heme to biliverdin, and of biliverdin to PCB or P $\phi$ B, respectively (27). The successful production of holo-phytochrome was already shown in bacteria, mammalian cells and the yeast *Pichia pastoris* (27–29), but not yet in *S. cerevisiae*. To change this, we integrated different combinations and versions of HOs and BRs into RL\_CT\_GI cells to detect the best chromophore-producing combination by measuring the reporter output (Figure 5B). The highest fold induction ( $\sim 3.5$ ) was achieved with the combinations of HY1 and PcyA, MTS-mHY1/MTS-mHY2, MTS-

mHY1/MTS-PcyA, and MTS-mHmx1/MTS-mHY2 (Figure 5D). In contrast to published data (28,29), targeting HY1 and PcyA to mitochondria did not gravely boost induction rates compared to cells expressing the two enzymes in the cytoplasm. Still, by combining native HY1 and PcyA we achieved robust expression and doubled the fold induction compared to RL\_CT\_GI without PCB supply. Furthermore, the difference to RL\_CT\_GI cells grown in medium supplemented with 25  $\mu$ M PCB (4.5-fold induction) was minor, demonstrating that we had established a system that works without an exogenous supply of the chromophore.

Chromophore biosynthesis genes *HY1* and *PcyA* were integrated into the genome of PhiReX 1.0 cells, resulting in the red light-dependent expression system PhiReX 1.0+, which does not require the supply of exogenous chromophore. With respect to expression output and fold induction, PhiReX 1.0+ shows a similar behavior as PhiReX 1.0 with supplied PCB. As compared to the galactose-inducible production of yEGFP, PhiReX 1.0+ results in similar fold induction values, but by far exceeds the absolute fluorescence values (Figure 6A). Users wishing to tightly control GOI expression in uninduced conditions may refer to PhiReX 1.1, which offers greatly reduced basal activity. Our analyses further demonstrate that the applied red light dose is a user-friendly option to easily fine-tune expression output, which is an important advantage over e.g. the *GALI* system (Figure 6B). The reversible control of gene expression by red/far-red light application has many potential implications for the construction of expression switches within synthetic regulatory networks (Figure 6C).

Importantly, while the requirement for the expensive and photolabile chromophore PCB may be a limiting factor for use in biotechnological applications in large-scale fermentations (49), our PhiReX system may overcome such limitations by producing the chromophore (PCB) intracellularly. However, a successful application of PhiReX in industrial settings most likely requires further (technical) improvements related to e.g. the light conditions available within a bio-fermenter and the light sources employed. In particular, in large, high-density cultures it may be challenging to activate gene expression by light in a sufficiently large number of cells. Nevertheless, as the PhyB/PIF3 interaction employed in PhiReX can be activated by short red light pulses and is stable over hours in the dark, we assume that continuous red light application in a stirred bioreactor is sufficient to activate all cells within a short time. As red light has only negligible effects on yeast cells (50), increasing the duration or intensity of red light irradiation may be a feasible approach to take.

Taken together, PhiReX allows for a tightly regulated and red light-dependent control of gene expression with a strong and robust fold induction. With a single cloning step the user can exchange the plasmid-located yEGFP reporter with the CDS of any GOI and thereby adopt the system easily to individual demands. Furthermore, the synTALE-based approach enables the user to flexibly program the PhiReX system towards any desired promoter region. As *S. cerevisiae* was engineered to produce sufficient amounts of the chromophore, the system is independent of the supply of toxic or expensive chemicals. PhiReX allows tunable and reversible induction via simple light exposure. We chose bud-

ding yeast, known to be well suited for pathway engineering and high protein production, as the host organism. We envisage that the fast, flexible, easy-to-use, nontoxic and low-cost nature of PhiReX makes it even suitable for industry-scale protein production.

## AVAILABILITY

Plasmids pRL\_CT\_GI-del1, pRL\_GI\_PCB28 and pRL\_yEGFP\_hc are available from Addgene ([www.addgene.org](http://www.addgene.org)). All other strains and plasmids reported in this study are available upon request from our laboratory.

## SUPPLEMENTARY DATA

Supplementary Data are available at NAR Online.

## ACKNOWLEDGEMENTS

L.H. thanks the Potsdam Graduate School for providing a scholarship. The authors greatly acknowledge Dr Pamela Holzlöhner (University of Potsdam, Germany) for introduction to flow cytometer.

*Author contributions.* L.H. designed and developed the overall strategy with contributions from F.M. L.H. conducted the experiments, analyzed the data and wrote the manuscript. F.M. provided and characterized the synTALE-DBD/BS pair and assisted with Cas9 genome editing. B.M.-R. initiated the project and the overall research strategy. B.M.-R. and F.M. edited the paper. All work was carried out in the Cell2Fab lab, led by K.M. All authors take full responsibility for the content of the paper.

## FUNDING

Federal Ministry of Education and Research of Germany (BMBF) [031A172]; Potsdam Graduate School. Funding for open access charge: BMBF [031A172].

*Conflict of interest statement.* None declared.

## REFERENCES

- Engels, B., Dahm, P. and Jennewein, S. (2008) Metabolic engineering of taxadiene biosynthesis in yeast as a first step towards Taxol (Paclitaxel) production. *Metab. Eng.*, **10**, 201–206.
- Ro, D.-K., Paradise, E.M., Ouellet, M., Fisher, K.J., Newman, K.L., Ndungu, J.M., Ho, K.A., Eachus, R.A., Ham, T.S. and Kirby, J. (2006) Production of the antimalarial drug precursor artemisinic acid in engineered yeast. *Nature*, **440**, 940–943.
- Galanie, S., Thodey, K., Trenchard, I.J., Interrante, M.F. and Smolke, C.D. (2015) Complete biosynthesis of opioids in yeast. *Science*, **349**, 1095–1100.
- Runguphan, W. and Keasling, J.D. (2014) Metabolic engineering of *Saccharomyces cerevisiae* for production of fatty acid-derived biofuels and chemicals. *Metab. Eng.*, **21**, 103–113.
- Si, T., Luo, Y., Xiao, H. and Zhao, H. (2014) Utilizing an endogenous pathway for 1-butanol production in *Saccharomyces cerevisiae*. *Metab. Eng.*, **22**, 60–68.
- Brat, D., Weber, C., Lorenzen, W., Bode, H.B. and Boles, E. (2012) Cytosolic re-localization and optimization of valine synthesis and catabolism enables increased isobutanol production with the yeast *Saccharomyces cerevisiae*. *Biotechnol. Biofuels*, **5**, 65.
- Macreadie, I.G., Horaitis, O., Verkuylen, A.J. and Savin, K.W. (1991) Improved shuttle vectors for cloning and high-level  $\text{Cu}^{2+}$ -mediated expression of foreign genes in yeast. *Gene*, **104**, 107–111.

8. Kramer, R.A., DeChiara, T.M., Schaber, M.D. and Hilliker, S. (1984) Regulated expression of a human interferon gene in yeast: control by phosphate concentration or temperature. *Proc. Natl. Acad. Sci. U.S.A.*, **81**, 367–370.
9. Belli, G., Gari, E., Piedrafita, L., Aldea, M. and Herrero, E. (1998) An activator/repressor dual system allows tight tetracycline-regulated gene expression in budding yeast. *Nucleic Acids Res.*, **26**, 942–947.
10. Quintero, M.J., Maya, D., Arévalo-Rodríguez, M., Cebolla, Á and Chávez, S. (2007) An improved system for estradiol-dependent regulation of gene expression in yeast. *Microb. Cell Factories*, **6**, 1.
11. Butt, T.R., Sternberg, E.J., Gorman, J.A., Clark, P., Hamer, D., Rosenberg, M. and Crooke, S.T. (1984) Copper metallothionein of yeast, structure of the gene, and regulation of expression. *Proc. Natl. Acad. Sci. U.S.A.*, **81**, 3332–3336.
12. Cherest, H., Kerjan, P. and Surdin-Kerjan, Y. (1987) The *Saccharomyces cerevisiae* *MET3* gene: nucleotide sequence and relationship of the 5' non-coding region to that of *MET25*. *Mol. Gen. Genet. MGG*, **210**, 307–313.
13. Shimizu-Sato, S., Hug, E., Tepperman, J.M. and Quail, P.H. (2002) A light-switchable gene promoter system. *Nat. Biotechnol.*, **20**, 1041–1044.
14. Hughes, R.M., Bolger, S., Tapadia, H. and Tucker, C.L. (2012) Light-mediated control of DNA transcription in yeast. *Methods*, **58**, 385–391.
15. Kennedy, M.J., Hughes, R.M., Peteya, L.A., Schwartz, J.W., Ehlers, M.D. and Tucker, C.L. (2010) Rapid blue-light-mediated induction of protein interactions in living cells. *Nat. Methods*, **7**, 973–975.
16. Sorokina, O., Kapus, A., Terecskei, K., Dixon, L.E., Kozma-Bognar, L., Nagy, F. and Millar, A.J. (2009) A switchable light-input, light-output system modelled and constructed in yeast. *J. Biol. Eng.*, **3**, 1.
17. Khalil, A.S., Lu, T.K., Bashor, C.J., Ramirez, C.L., Pyenson, N.C., Joung, J.K. and Collins, J.J. (2012) A synthetic biology framework for programming eukaryotic transcription functions. *Cell*, **150**, 647–658.
18. Farzadfard, F., Perli, S.D. and Lu, T.K. (2013) Tunable and multifunctional eukaryotic transcription factors based on CRISPR/Cas. *ACS Synth. Biol.*, **2**, 604–613.
19. Blount, B.A., Weenink, T., Vasylychko, S. and Ellis, T. (2012) Rational diversification of a promoter providing fine-tuned expression and orthogonal regulation for synthetic biology. *PLoS One*, **7**, e33279.
20. Ni, M., Tepperman, J.M. and Quail, P.H. (1999) Binding of phytochrome B to its nuclear signalling partner PIF3 is reversibly induced by light. *Nature*, **400**, 781–784.
21. Boch, J. and Bonas, U. (2010) *Xanthomonas* AvrBs3 family-type III effectors: discovery and function. *Phytopathology*, **48**, 419.
22. Boch, J., Scholze, H., Schornack, S., Landgraf, A., Hahn, S., Kay, S., Lahaye, T., Nickstadt, A. and Bonas, U. (2009) Breaking the code of DNA binding specificity of TAL-type III effectors. *Science*, **326**, 1509–1512.
23. Moscou, M.J. and Bogdanove, A.J. (2009) A simple cipher governs DNA recognition by TAL effectors. *Science*, **326**, 1501–1501.
24. Kunkel, T., Neuhaus, G., Batschauer, A., Chua, N.H. and Schäfer, E. (1996) Functional analysis of yeast-derived phytochrome A and B phycocyanobilin adducts. *Plant J.*, **10**, 625–636.
25. Kunkel, T., Speth, V., Büche, C. and Schäfer, E. (1995) *In vivo* characterization of phytochrome-phycocyanobilin adducts in yeast. *J. Biol. Chem.*, **270**, 20193–20200.
26. Li, L. and Lagarias, J.C. (1994) Phytochrome assembly in living cells of the yeast *Saccharomyces cerevisiae*. *Proc. Natl. Acad. Sci. U.S.A.*, **91**, 12535–12539.
27. Gambetta, G.A. and Lagarias, J.C. (2001) Genetic engineering of phytochrome biosynthesis in bacteria. *Proc. Natl. Acad. Sci. U.S.A.*, **98**, 10566–10571.
28. Müller, K., Engesser, R., Timmer, J., Nagy, F., Zurbriggen, M.D. and Weber, W. (2013) Synthesis of phycocyanobilin in mammalian cells. *Chem. Commun.*, **49**, 8970–8972.
29. Shin, A.Y., Han, Y.J., Song, P.S. and Kim, J.I. (2014) Expression of recombinant full-length plant phytochromes assembled with phytochromobilin in *Pichia pastoris*. *FEBS Lett.*, **588**, 2964–2970.
30. Levsikaya, A., Chevalier, A.A., Tabor, J.J., Simpson, Z.B., Lavery, L.A., Levy, M., Davidson, E.A., Scouras, A., Ellington, A.D., Marcotte, E.M. et al. (2005) Synthetic biology: engineering *Escherichia coli* to see light. *Nature*, **438**, 441–442.
31. Hochrein, L., Machens, F., Gremmels, J., Schulz, K., Messerschmidt, K. and Mueller-Roeber, B. (2017) AssemblX: A user-friendly toolkit for rapid and reliable multi-gene assemblies. *Nucleic Acids Res.*, gkx034.
32. Ellis, T., Wang, X. and Collins, J.J. (2009) Diversity-based, model-guided construction of synthetic gene networks with predicted functions. *Nat. Biotechnol.*, **27**, 465–471.
33. Maeder, M.L., Linder, S.J., Cascio, V.M., Fu, Y., Ho, Q.H. and Joung, J.K. (2013) CRISPR RNA-guided activation of endogenous human genes. *Nat. Methods*, **10**, 977–979.
34. Zhang, Y., Werling, U. and Edlmann, W. (2012) SLiCE: a novel bacterial cell extract-based DNA cloning method. *Nucleic Acids Res.*, **40**, e55.
35. Gibson, D.G., Young, L., Chuang, R.-Y., Venter, J.C., Hutchison, C.A. and Smith, H.O. (2009) Enzymatic assembly of DNA molecules up to several hundred kilobases. *Nat. Methods*, **6**, 343–345.
36. Kouprina, N. and Larionov, V. (2006) TAR cloning: insights into gene function, long-range haplotypes and genome structure and evolution. *Nat. Rev. Genet.*, **7**, 805–812.
37. Gietz, R.D. and Schiestl, R.H. (2007) High-efficiency yeast transformation using the LiAc/SS carrier DNA/PEG method. *Nat. Protoc.*, **2**, 31–34.
38. Morbitzer, R., Elsaesser, J., Hausner, J. and Lahaye, T. (2011) Assembly of custom TALE-type DNA binding domains by modular cloning. *Nucleic Acids Res.*, **39**, 5790–5799.
39. DiCarlo, J.E., Norville, J.E., Mali, P., Rios, X., Aach, J. and Church, G.M. (2013) Genome engineering in *Saccharomyces cerevisiae* using CRISPR-Cas systems. *Nucleic Acids Res.*, gkt135.
40. Rodríguez-López, M., Cotobal, C., Fernández-Sánchez, O., Bravo, N.B., Oktriani, R., Abendroth, H., Uka, D., Hoti, M., Wang, J. and Zaratigui, M. (2016) A CRISPR/Cas9-based method and primer design tool for seamless genome editing in fission yeast. *Wellcome Open Res.*, **1**, 19.
41. Van den Ackerveken, G., Marois, E. and Bonas, U. (1996) Recognition of the bacterial avirulence protein AvrBs3 occurs inside the host plant cell. *Cell*, **87**, 1307–1316.
42. Pfeiffer, A., Nagel, M.-K., Popp, C., Wüst, F., Bindics, J., Viczián, A., Hiltbrunner, A., Nagy, F., Kunkel, T. and Schäfer, E. (2012) Interaction with plant transcription factors can mediate nuclear import of phytochrome B. *Proc. Natl. Acad. Sci. U.S.A.*, **109**, 5892–5897.
43. Beyer, H.M., Juillot, S., Herbst, K., Samodelov, S.L., Müller, K., Schamel, W.W., Roömer, W., Schäfer, E., Nagy, F. and Straähle, U. (2015) Red light-regulated reversible nuclear localization of proteins in mammalian cells and zebrafish. *ACS Synth. Biol.*, **4**, 951–958.
44. Chen, M., Tao, Y., Lim, J., Shaw, A. and Chory, J. (2005) Regulation of phytochrome B nuclear localization through light-dependent unmasking of nuclear-localization signals. *Curr. Biol.*, **15**, 637–642.
45. Ponka, P. (1999) Cell biology of heme. *Am. J. Med. Sci.*, **318**, 241–256.
46. Konermann, S., Brigham, M.D., Trevino, A.E., Hsu, P.D., Heidenreich, M., Cong, L., Platt, R.J., Scott, D.A., Church, G.M. and Zhang, F. (2013) Optical control of mammalian endogenous transcription and epigenetic states. *Nature*, **500**, 472–476.
47. Szurek, B., Marois, E., Bonas, U. and Van den Ackerveken, G. (2001) Eukaryotic features of the *Xanthomonas* type III effector AvrBs3: protein domains involved in transcriptional activation and the interaction with nuclear import receptors from pepper. *Plant J.*, **26**, 523–534.
48. Matsushita, T., Mochizuki, N. and Nagatani, A. (2003) Dimers of the N-terminal domain of phytochrome B are functional in the nucleus. *Nature*, **424**, 571–574.
49. Salinas, F., Rojas, V., Delgado, V., Agosin, E. and Larrondo, L.F. (2017) Optogenetic switches for light-controlled gene expression in yeast. *Appl. Microbiol. Biotechnol.*, 1–12.
50. Robertson, J.B., Davis, C.R. and Johnson, C.H. (2013) Visible light alters yeast metabolic rhythms by inhibiting respiration. *Proc. Natl. Acad. Sci. U.S.A.*, **110**, 21130–21135.